Tribology of dual Pickering double emulsions: Machine learning-aided inner droplet analysis

Food Hydrocolloids 172 (2026) 112035

Contents lists available at ScienceDirect

Food Hydrocolloids

journal homepage: www.elsevier.com/locate/foodhyd

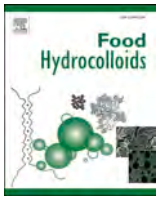

Tribology of dual Pickering double emulsions: Machine learning-aided inner droplet analysis

Elizabeth Tenorio-Garcia [a], Siavash Soltanahmadi [a], Jens Saalbrink [c,d], Jose C. Bonilla [c,d], Michael Rappolt [a], Elena Simone [a,b], Anwesha Sarkar [a,*]

[a] Food Colloids and Bioprocessing Group, School of Food Science and Nutrition, University of Leeds, Leeds, LS2 9JT, UK
[b] Department of Applied Science and Technology (DISAT), Politecnico di Torino, Torino, 10129, Italy
[c] Department of Green Technology, University of Southern Denmark, DK-5230, Odense M, Denmark
[d] Department of Food Science, University of Copenhagen, DK-1958, Frederiksberg C, Denmark

ARTICLE INFO

Keywords:
Water-in-oil emulsion
Cocoa butter
Microgel
AI-Assisted image analysis
Tongue
Friction

ABSTRACT

This study investigated the tribological performance of Pickering water-in-oil emulsions and dual Pickering water-in-oil-in-water double emulsions (DEs) stabilized with particles at both the interfaces. W/O emulsions were stabilized by cocoa butter-based oleogel (CBolg) crystals, while DEs incorporating these emulsions were stabilized by whey protein microgels (WPM). The influence of temperature (21 and 37 °C) and surface texture (smooth *vs* biomimetic tongue-like surface) were investigated in tribology of W/O emulsions (30–60 % v/v water) and DEs (with 20 and 60 wt% W/O phase). In smooth surfaces, CBolg played a critical role in reducing the friction coefficient (μ) primarily via a fat-driven lubrication mechanism that was temperature dependent. While in DEs, smaller oil droplets encapsulating water provided similar lubrication to oil-based systems until starvation occurred. Strikingly, the water content in W/O emulsions exhibited distinct differences between emulsion systems within the biomimetic tongue-like surfaces, demonstrating lower lubricity at higher water concentration. Confocal microscopy images analyzed using Machine Learning (ML)-supported droplet segmentation enabled a more precise evaluation of structural changes within DEs when subjected to tribological stress. We demonstrated that although changes in inner droplet size altered in DEs, their contribution to the overall lubrication performance was minimal, due to their limited entrainment. Of more importance, the tribological performance was governed by the WPM with minimal influence from the droplet-entrained phenomena. These fundamental insights highlight the relevance of structured water in understanding frictional performance in emulsified systems, with structural integrity, composition, and topography of the tribological surface emerging as key factors.

1. Introduction

Fat contributes to multiple desirable physicochemical properties and sensory characteristic of food products, hence, reducing fat content has been a long-standing challenge in food industry (Kew et al., 2020). For example, decreasing the volume fraction of oil droplets in oil-in-water (O/W) emulsions leads to viscosity reduction and diminished spreadability as the product becomes more fluid, losing its gel-like properties (McClements, 2015). Many food products, such as sauces, mayonnaise, milk, dressings are O/W emulsions or contain ingredients that are emulsions, where fat exists in the form of oil droplets. In this context, double emulsions (DEs) present a promising alternative for reducing fat content while maintaining structural integrity where part of the fat is replaced by water droplets.

DEs are complex multiphasic dispersions consisting of larger droplets, containing smaller dispersed droplets of a different phase. One example of DEs are water-in-oil-in-water (W/O/W) emulsions, in which oil droplets encapsulate smaller water droplets. However, DEs, are in general more susceptible to destabilization compared to single W/O emulsions. As multiphasic systems, DEs face challenges in maintaining stability in both the inner and outer droplets. Pickering stabilization has been shown to significantly enhance the stability of emulsions via creating particle-stabilized interface offering high desorption energies and hence droplets are resistant to coalescence and Ostwald ripening (Sarkar & Dickinson, 2020). Despite ongoing efforts, few studies have applied Pickering stabilization to DEs using only natural sources; this is

* Corresponding author.
E-mail address: A.Sarkar@leeds.ac.uk (A. Sarkar).

https://doi.org/10.1016/j.foodhyd.2025.112035
Received 12 June 2025; Received in revised form 29 August 2025; Accepted 24 September 2025
Available online 26 September 2025

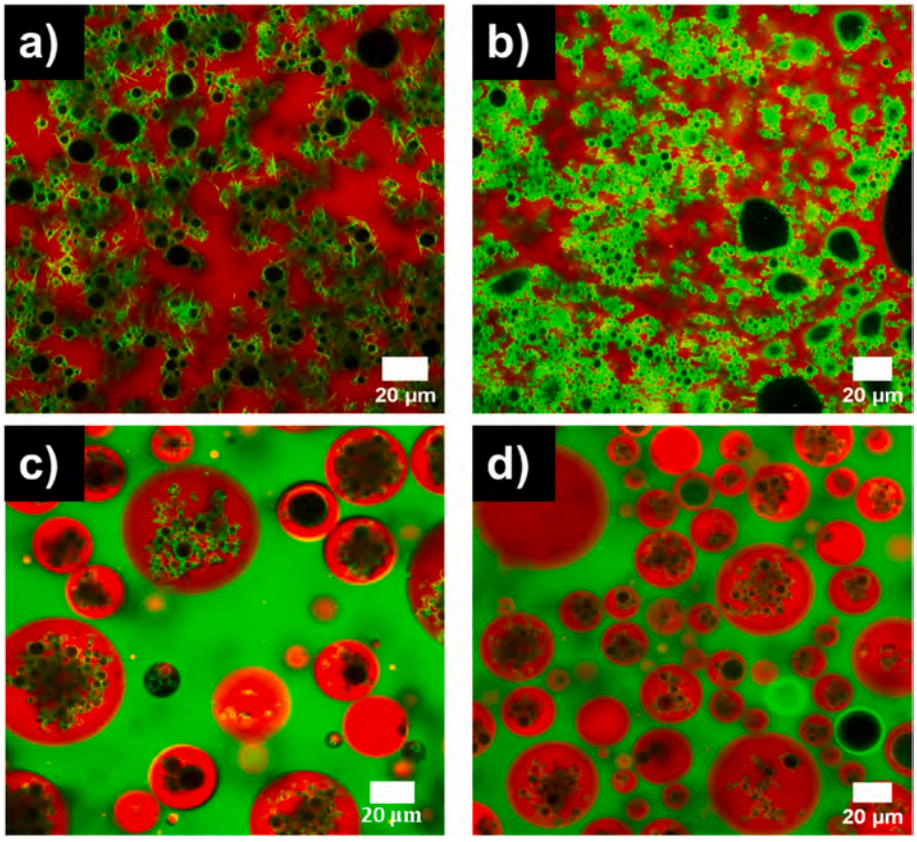

Fig. 1. Pickering-stabilized W/O single emulsions (SEs) with 30 % v/v (**a**) and 60 % v/v water content (**b**). Dual-Pickering-stabilized W/O/W double emulsions (DEs) containing 20 wt% (**c**) and 50 wt% (**d**) of W/O SEs, stabilized with CBolg. CB crystals depicted in green, surround the small black water droplets, while whey protein microgels (WPM), also fluorescent in green, are distributed in the continuous water phase. The oil phase, in contrast, is fluorescent in red. (For interpretation of the references to colour in this figure legend, the reader is referred to the Web version of this article.)

because there is a limited availability of particles capable of stabilizing the water/oil interface (Spyropoulos et al., 2019; Tenorio-Garcia, et al., 2022, 2024; Zembyla et al., 2019).

Besides stability, consumer acceptance is key to dictating a product's success and repeated consumption. Any modification to food formulation is likely to alter the sensory properties. While sensory evaluation typically involves expert panels and consumer testing (Ares & Varela, 2017), these methods can be time-consuming, particularly during the design phase. Rheology and tribology techniques offer efficient quantitative proxies for assessing intrinsic product parameters, providing valuable insights in a shorter timeframe to accelerate product development particularly in the initial phases (Sarkar & Krop, 2019). Tribology and rheology have emerged as key tools for elucidating textural perception of food systems and establishing connections between sensory and instrumental data. While rheology focuses on bulk deformation and flow properties, these measurements often do not capture the sensory characteristics perceived in thin-films, such as creaminess, smoothness, slipperiness (J. Chen & Stokes, 2012). Classical tribology examines surface interactions at close proximity, defined by three regimes – boundary, mixed and hydrodynamic – ranging from direct surface contact to complete separation by a continuous fluid film, as depicted by Stribeck curves (Sarkar, Andablo-Reyes et al., 2019). In recent years, there has being growing research on developing Pickering double emulsions stabilized by natural particles (Du & Meng, 2025; Li et al., 2021; Tenorio-Garcia et al., 2024), but understanding their tribological properties remains largely unexplored. Studies indicate that the type of emulsion, particle nature, droplet size and the external concentration of the dispersed phase significantly influence the frictional behavior (Araiza-Calahorra et al., 2024; Bao et al., 2021; M. Chen, Abdullah, et al., 2022; Du et al., 2024).

With recent advancement in 3D-printing, surfaces that closely mimic the human tongue, incorporating mechanical properties, wettability characteristics and surface textures are available that more accurately mimic the human oral surfaces bringing mechanistic insights about the sensorial consequences (Andablo-Reyes et al., 2020; Soltanahmadi et al., 2022; Qi Wang, Zhu, & Chen, 2021). To our knowledge, this is the first study that systematically examines the tribological performance of Pickering W/O emulsions and DEs in human tongue-like surface.

Hence, the aim of this study was to investigate the tribology properties of complex colloidal systems, *i.e.*, dual Pickering DEs developed using cocoa butter-based oleogel crystals and microgel particles using biomimetic tongue-like surface. Firstly, this study examined the tribological effect of structuring oil into oleogels and then single W/O single emulsions with varying droplet volume fractions (30–60 % v/v water) to set the scene. Then, W/O/W DEs that incorporate the crystalline network of oleogels and microgels at the interface of the DEs containing 20 and 60 wt% W/O phase were examined for their tribological performance. Additionally, influence of temperature of production (21 °C) versus oral processing temperature (37 °C) was investigated. To provide further insight, all the systems and conditions were tested applying a tongue-mimicked surface to elucidate the effects of surface properties on friction in scenarios that closely resemble oral processing and compared with smooth surfaces. Finally, to understand the effect on tribological shear on inner droplets of DEs, image analysis assisted by machine learning (ML) algorithms was employed to pinpoint any difference in droplet size distribution affecting the tribological performance.

2. Materials and methods

2.1. Materials

Refined, bleached, and deodorized cocoa butter (CB) and high oleic sunflower oil (HOSO) were obtained from Cargill (UK). The typical composition of the fatty acids present in CB was 36 % stearic acid, 34 % oleic acid, 26 % palmitic acid, 2.7 % linoleic acid, and 0.9 % arachidic acid by weight. Meanwhile, HOSO typically contained 86 % oleic acid, 5 % stearic acid, 3 % linoleic acid, 3 % palmitic acid, 1.5 % behenic acid, and 0.7 % arachidic acid by weight (Metilli et al., 2021). Sodium phosphate monobasic monohydrate, sodium phosphate dibasic anhydrous, and hydroxyl chloride were purchased from Thermo Fisher Scientific Loughborough, UK. Sodium azide was obtained from Sigma Aldrich (USA) and used as an antibacterial agent at 0.02 %. Whey protein isolate powder (WPI) containing ≥90 % protein was kindly donated by Fonterra Limited (Auckland, New Zealand). Phosphate buffer was prepared in Milli-Q water with a resistivity of 18 MΩ cm (Milli-Q apparatus, Millipore Corp., Bedford, MA, USA).

2.2. Preparation of Pickering particles

The methodology for preparing the particles has been described previously (Tenorio-Garcia, et al., 2023, 2024). Cocoa butter oleogel crystals (CBolg) were utilized to stabilize the single Pickering water-in-oil (W/O) emulsion. Briefly, cocoa butter (CB) and high oleic sunflower oil (HOSO) were mixed at 55 °C for 30 min to create a 10 % wt CB blend, which was then cooled under controlled conditions to form a structured oleogel containing CB crystals in the β(v) polymorphic form (Tenorio-Garcia et al., 2023). After crystallization reached equilibrium, the temperature was adjusted to 20 °C, a critical factor for emulsion stability due to the low melting point of CBolg (23 °C) (Metilli et al., 2021; Tenorio-Garcia et al., 2023).

For the oil-water interface stabilization, sub-micron whey protein microgel (WPM) were employed. A 10 wt% dispersion of whey protein isolate (WPI) was prepared in 20 mM phosphate buffer and stirred for 2 h at room temperature, allowing complete dissolution and hydration of the proteins (Sarkar et al., 2017). This solution was then heated to 90 °C for 30 min, followed by a cooling step at room temperature for 15 min and storage at 4 °C overnight to form a WPI hydrogel. The hydrogel was diluted with buffer in 50 v/v% and broken into macrogel fragments using a hand blender (HB724, Kenwood, UK) for 1 min to form a dispersion of macroscopic hydrogel particles containing 5.0 wt% WPI (or 50 vol% WPM). The resulting dispersion was passed twice through a high-pressure homogenizer at 250 bar to reduce particle size to form whey protein microgel (WPM) (Panda Plus, GEA Niro Soave, Parma, Italy). The resulting WPM with 5.0 wt% protein (a 50 % v/v WPM in the dispersio) were used to stabilize the secondary emulsion of the W/O/W DEs.

2.3. Fabrication of W/O emulsions and W/O/W emulsions (DEs)

The continuous phase of W_1/O emulsions consisted solely of CBolgs without surfactant addition and the dispersed phase was phosphate buffer (20 mM at pH 7.0). The dispersed phase was precooled to 4 °C in an ice bath for 2 h. The cold water ensured a controlled processing temperature of 21 °C during emulsification. Single emulsions were prepared by mixing the cold-water phase with the CBolgs and emulsifying with a rotor-stator emulsifier (Ultra-Turrax S25N-18G, IKA, Staufen) at 24,000 rpm for 40 s within a temperature-controlled vessel set at 21 °C to match the temperature for crystal formation (10 v/v% CB). Different concentrations of water in W/O emulsions (30 %, 50 % and 60 % v/v) were used to evaluate effect of the water on the tribological properties of the W/O emulsions (Fig. 1a–b).

The $W_1/O/W_2$ emulsion (DEs) was made by the two-step process using the resulting W_1/O emulsion, which was used as the dispersed phase to form the secondary O/W_2 emulsion, resulting in a $W_1/O/W_2$ double emulsion. Once the single emulsion was formed, it was added to the continuous phase containing WPM to create dual Pickering DEs. The name "dual" is used here to indicate the presence of Pickering particles *i.e.* CBolgs in the W_1/O and WPM in the O/W_2 phase (Tenorio-Garcia et al., 2024). The DEs were made in the jacketed vessel connected to a Huber Ministat 125 thermostat (Huber Germany), maintaining the working temperature (21 °C) of the single emulsion, and emulsifying with the secondary water phase in a rotor-stator emulsifier (Ultra-Turrax S25N-18G, IKA, Staufen) 11,000 rpm for 40 s. Finally, the DEs were stored at a controlled temperature of 21 °C. Two DEs with different oil phase (W_1/O) volume fractions were prepared: one with a 20/80 oil (W_1/O)-to-water ratio (resulting in a final composition of 6/14/80) and another with a 50/50 oil (W_1/O)-to-water ratio (resulting in a final composition of 15/35/50). The water volume fraction of the W_1/O emulsion was kept the same in the $W_1/O/W_2$ emulsions, being 30/70 throughout all the experiments (Fig. 1c–d). For clarity in the discussion, these emulsions are referred to as 20DEs and 50DEs, respectively. It is important to note that the internal water ratio represents an ideal estimation, as some water droplets may break and migrate to the external phase during the homogenization process.

2.4. Apparent viscosity

Rheological measurements of both the single W/O emulsions and DEs were conducted using a modular compact rheometer MCR 302 stress-controlled (Anton Paar, Austria), with shear rates ranging from 0.1 to 2500 s^{-1}. Measurements were taken approximately 10 min after emulsion preparation. A concentric cylinder geometry (CC27/T200/SS) was employed for all test, with approximately 10 ml of each sample used. It is important to note that the W/O emulsions (50 % and 60 % v/v water) exhibited a more gel-like consistency. Viscosity was measured at two different temperatures, 21 °C and 37 °C, to ensure stable conditions for the CBolg and to simulate oral physiological conditions, respectively. Samples were allowed to equilibrate for 5–10 min at each respective temperature. At least three replicates were performed on separate samples, and the data were averaged using OriginPro software (Average multiple curves).

2.5. Preparation of 3D-tongue-mimicking elastomeric surfaces

The 3D-tongue-mimicking surface was designed to replicate the stiffness, roughness and hydrophilicity of a real human tongue (Andablo-Reyes et al., 2020). The surface was engineered to randomly place 200 filiform-shaped cylindrical rods with dome head, each with a height of 250 μm and a radius of 175 μm, alongside 20 fungiform-shaped hemispheres measuring of 500 μm in both height and radius. The AutoCAD® design was 3D printed onto acrylic resin (Perfactory® HTM140) using a Perfactory 3D Printer, resulting in a master mould that would serve as the template for producing all the tongues replicas required for the study. Detailed characteristics of the elastomer surface can be found in previous studies (Andablo-Reyes et al., 2020; Soltanahmadi et al., 2022).

Briefly, the fabrication of the 3D-tongue-mimicking surface followed a soft-lithographic process using a master mould. The biomimetic tongue was fabricated using a mixture of Ecoflex® Part A and Part B in a 1:1 ratio. To retard the curing process, 0.1 w/w% of Slo-Jo™ retarder was incorporated into fresh Ecoflex® Part B and thoroughly mixed before adding Part A. Subsequently, 0.05 w/w% Span 80 was added to the mixture and hand-stirred for 1 min. A total of 7.1 g of the resulting mixture was then poured into the mould. The mould was placed under vacuum at 200 psi for 30 min to remove air bubbles and ensure proper filling of the small cavities in the mould replicating filiforms and fungiforms. The polymer mixture was cured at room temperature for 48 h. Once cured, the elastomeric replica was carefully peeled off the mould and cleaned using sonication for 5 min to remove any residual material

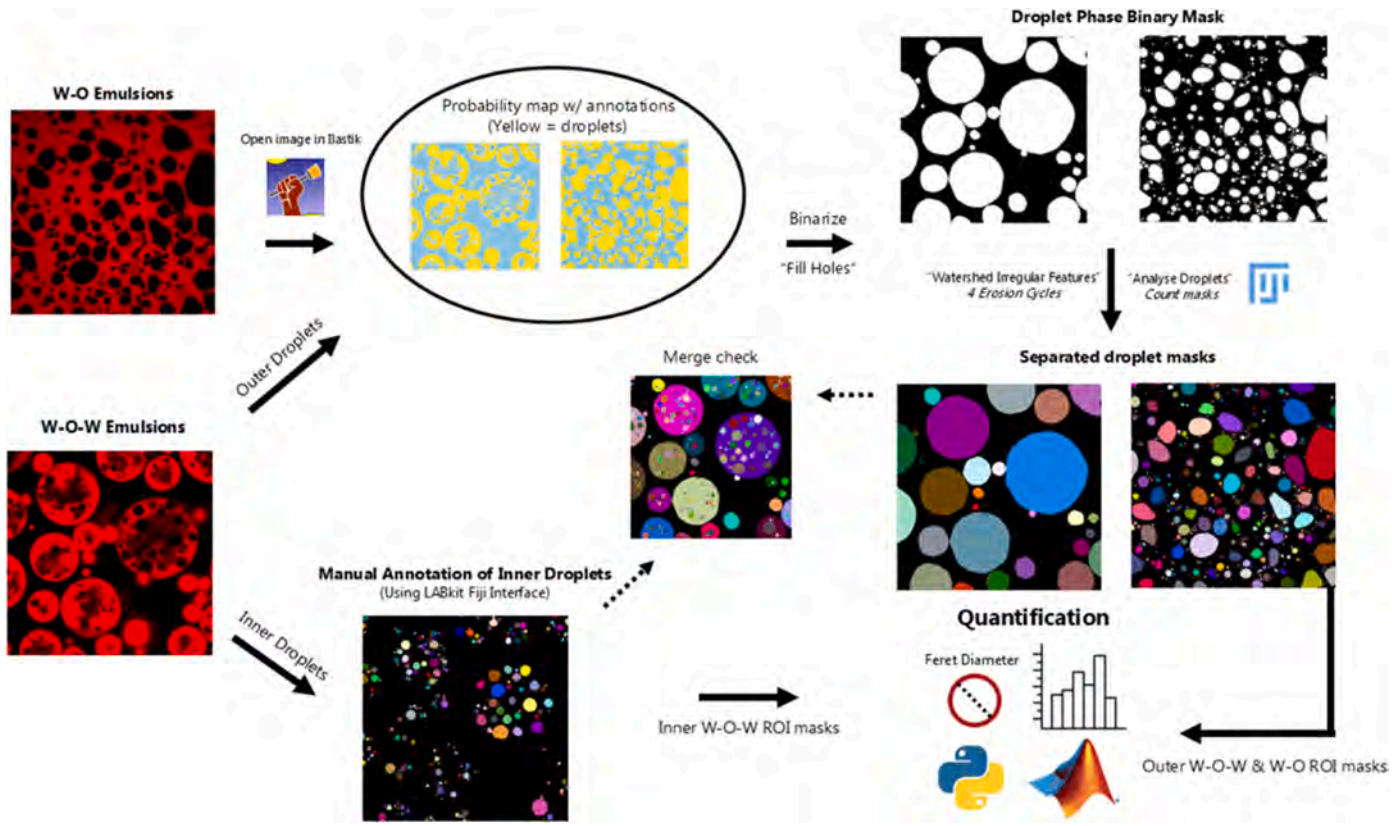

Fig. 2. Schematic representation of the methodology used to quantify water droplets in W/O single and both water and oil droplets in W/O/W double emulsion (DEs), using a combination of confocal microscopy and machine learning-based image analysis.

and contamination. The resulting elastomeric samples exhibited a random spatial distribution of filiform and fungiform papillae, modelled on the size and distribution characteristics observed in human tongue (Andablo-Reyes et al., 2020; Soltanahmadi et al., 2023).

2.6. Tribological setup

The frictional properties of the emulsion systems were investigated using two different experimental setups: the MTM2 tribometer (MTM2, PCS Instruments, London, UK) with smooth surfaces and a bespoke setup using a rheometer (MCR 302 Anton Paar, Austria) integrated with a biomimetic tongue-like surface. The modified rheometer setup enabled the measurement of the friction coefficient (μ) utilizing the previously described 3D-tongue-mimiched elastomer surface. The MTM2 has been used in this work as a benchmark as it is extensively used in literature for oral tribology studies. However, MTM2 cannot replicate the realistic tribological conditions in mouth in contrast to unique capability of the custom-designed setup exploiting the biomimetic tongue (Soltanahmadi et al., 2023).

The friction tests using the MTM2 tribometer were conducted in a ball-on-disk configuration, applying a slide-to-roll ratio (SRR) of 0.5. The setup utilized smooth polydimethylsioxane (PDMS) specimens (PCS Instruments, UK), *i.e.* a ball with a diameter of 19 mm and a disc with a diameter of 46 mm. The PDMS specimens had an elastic modulus of 2.1 MPa and surface roughness of 20 nm (Andablo-Reyes et al., 2019) and were used as received (i.e. with no surface treatment). A load of 2N was applied during experiments, corresponding to a Hertzian contact pressure of ~200 kPa (Sarkar, Andablo-Reyes et al., 2019). The friction coefficient (μ) results were measured in order of increasing speed from 0.00001 to 2.5 ms^{-1}.

The tribological properties of the samples were also evaluated using a biomimetic tongue surface. The experiment was conducted with a T-PID/44 MCR tribology cell (Anton Paar, Austria), which operates based on a pin-on-disc measuring principle. The tongue-mimicking surface was attached to the plastic plate of the tribology cell, secured by a metal ring, creating a reservoir for the testing materials (*i.e.* emulsions). The applied contact pressure was estimated at 40–50 kPa which is in the order of the realistic contact pressure between human tongue and palate during oral processing (Soltanahmadi et al., 2023). The μ results were recorded against entrainment speed in increasing order, ranging from 0.00001 to 2.5 ms^{-1}. Each emulsion sample was evaluated with at least one read on three distinct elastomeric specimens using fresh samples.

For both experimental setups, extensive cleaning procedures were employed between each test to eliminate any surface contamination. The specimens underwent sonication with various solutions, including soap or sodium dodecyl sulfate (for protein-containing solutions), followed by isopropyl alcohol (IPA) and distilled water for 10 min at each step. The friction coefficient was measured at two temperatures: 21 °C and 37 °C, the latter simulating oral conditions.

2.7. Microscopy

2.7.1. Confocal laser scanning microscopy (CLSM)

The morphology of the W/O emulsions and W/O/W DEs was examined using a Zeiss LSM 880 inverted microscope (Carl Zeiss MicroImaging GmbH, Jena, Germany). For initial imaging (*i.e.* before samples are subjected to tribological shear), the emulsions were stained with three different dyes to visualize various components within DEs and Pickering stabilization in the studied systems. Approximately 10 μL of a mixture containing Nile Red (1 mg/mL in dimethyl sulfoxide), Fast green (1 mg/mL in MilliQ water) and Nile blue (1 mg/mL in MilliQ water) were added to 1 g of the DEs. To investigate the effect of tribological forces on microstructural changes of emulsions, the samples were stained with Nile red alone which facilitated the distinction between the

water and oil phase. Staining of the emulsions and imaging were conducted immediately after preparation of samples or after tribological tests.

Emulsions were placed into a concave confocal microscope slide, covered with a glass coverslip, and observed with a 63 × oil immersion lens with pinhole maintained at 1 Air Unit to effectively filter out most of the light scattering. The wavelength used to excite Nile Red was 488 nm to illuminate oil phase in red, for Nile Blue 625 nm to illuminate CBolg crystals at the water-oil interface in green, while Fast Green was excited at a wavelength of 633 nm to illuminate WPM at the oil-water interface in green. Nile red (NR) staining oil was helpful in confirming the existence of DEs by revealing water droplets encapsulated within the oil droplets, visually represented as red droplets-stained with discernible dark regions which correspond to the internal water.

2.8. Image analysis

The confocal microscopy images from W/O emulsions and DEs (Fig. 1) were analyzed with image analysis as described by Saalbrink et al. (2025). The droplets in the images were segmented using the software Ilastik (Berg et al., 2019). In Ilastik, machine-learning models were trained through a pixel classification algorithm by manually annotating the image background and the droplets (Fig. 2). To ensure the droplets were segmented from the same criteria, the same number of annotations were done in the background and droplets for each emulsion treatment. The segmented binary images were subsequently exported into FIJI software (Schindelin et al., 2012). In the images from W/O emulsions, touching droplets were split by applying the functions "fill holes" and "watershed irregular features" using 4 erosion cycles. In the images of W/O/W emulsions, the inner and outer droplets were manually annotated in FIJI's lab kit plugin. For the inner droplets, only in-focus droplets were annotated. The sharpness of the edges of the droplets was used to differentiate between in-focus droplets and out-of-focus (blurry) droplets. Subsequently, the droplet count was acquired using the "analyze particles" function in FIJI (Fig. 2). Further, quantitative shape descriptors from each droplet were obtain by applying the function 'Label-Statistics' from the Simple-ITK library to the image mask containing the segmented droplets. This was done using Python programing language. From the obtained parameters, the 'Feret diameter' and 'area' of each droplet were imported into Matlab R2022b (Mathworks, USA) and plotted to visualize the size distribution of the droplets. Additionally, 'D90' values were calculated for each image.

2.9. Statistics

All quantitative results are based on three measurements on triplicate samples (n = 3 × 3) and data is represented as a mean and standard deviation. ANOVA statistics test was done using Minitab program. Means comparison was done by using the Tukey's test where statistical significance was noted at $p < 0.05$.

3. Results and discussion

To systematically analyze the tribological properties of DEs, we first examined the tribological behavior of the W/O emulsions as a function of the volume fraction of water droplets and their individual components, such as the oil (HOSO), oleogel (CBolg) and phosphate buffer (used as the dispersing phase). Secondly, we examined the complete DE systems as a function of volume fraction of W/O phase to shed light into how each component contributes to the overall lubrication behavior. In all cases, systems were tested using both MTM2 (smooth hydrophobic surface) and the setup with the textured, weakly polar, biomimetic tongue-like surface.

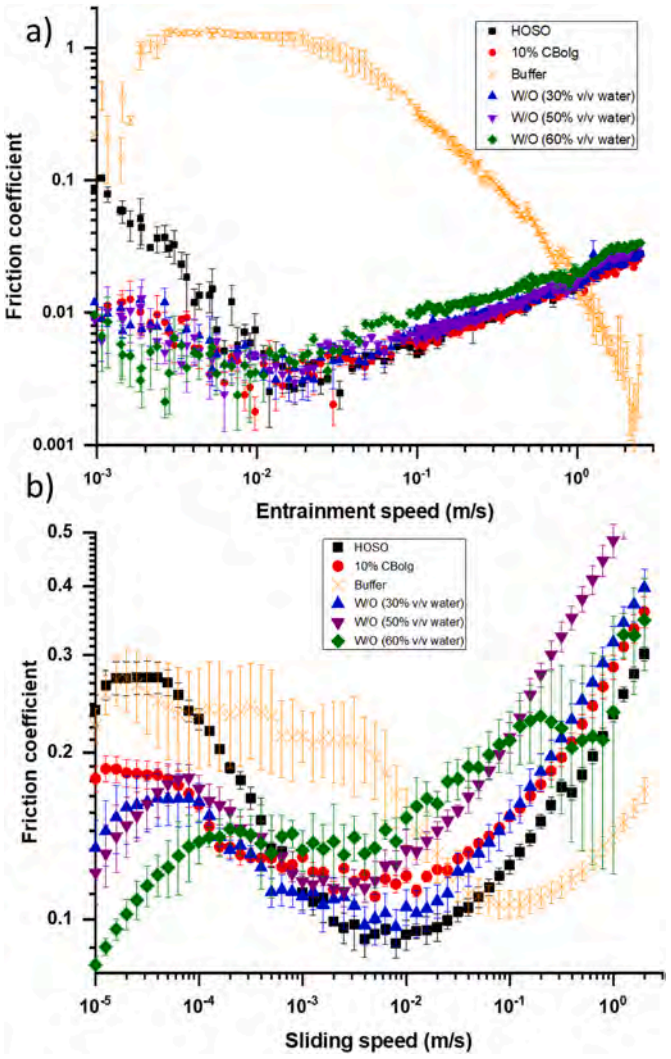

Fig. 3. Friction coefficient (μ) versus entrainment speed in smooth, hydrophobic polydimethylsiloxane (PDMS) contact surface (**a**) and sliding speed in textured, soft, biomimetic tongue-like surface (**b**), respectively for high oleic sunflower oil, 10 % v/v CB oleogel (CBolg), 10 mM phosphate buffer (Buffer), and W/O emulsions with varying water concentrations (30 % v/v, 40 % v/v, 50 % v/v, and 60 % v/v water). Measurements were conducted at 21 °C.

3.1. Soft tribology of the single Pickering W/O emulsions

3.1.1. Smooth hydrophobic surface

The friction results obtained for the W/O emulsions at 30 %, 50 % and 60 % v/v water and the respective emulsion components (*i.e.* HOSO, CBolg, phosphate buffer) are shown in Fig. 3a. The lubrication data of these components aligned with previous findings, in which CBolg and W/O emulsions demonstrated superior lubrication properties compared to the buffer and also HOSO alone (Douaire et al., 2014; Tecuanhuey et al., 2024). At speeds $<10^{-2}$ m/s, a seemingly mixed lubrication regime was observed for W/O emulsion, CBlog and HOSO samples. Now, separating each component of the single W/O emulsions revealed that structuring HOSO through the formation of a crystal network (CBolg) further decreased the friction coefficients (μ) at lower speeds as compared to liquid HOSO (Fig. 3a). As indicated by closely overlapped μ values across all speeds, CBlog was the protagonist in driving lubricity for the W/O samples and their ability to form a fluid film at the contact surface. Across all emulsion systems and CBolg (Fig. 3a), μ values were approximately 0.01 at low sliding speeds (0.001 m/s), decreasing by an order of magnitude to around 0.002 in the mixed lubrication regime.

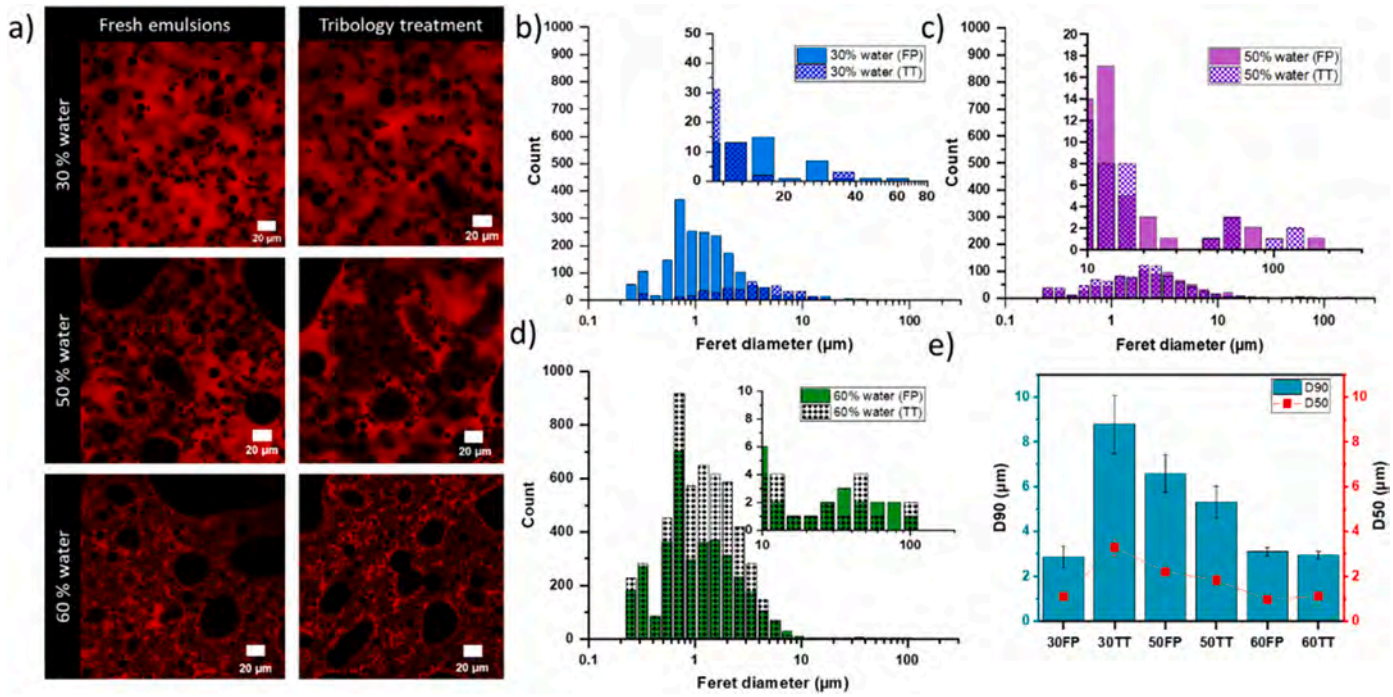

Fig. 4. Morphological evolution (**a**) of W/O emulsions before and after exposure to frictional forces in a biomimetic tongue-like surface at 21 °C. The droplet size distribution shows the microstructural changes in W/O emulsions with water concentrations of 30 % (**b**), 50 % (**c**), and 60 % (**d**) (v/v) and the distribution parameter D50 and D90 changes of all emulsions (**e**) before and after tribology obtained using machine learning. FP stands for the freshly prepared emulsions, while TT stands for post-tribology test.

At speeds $>10^{-2}$ m/s, exhibiting lubrication behaviors consistent with elasto-hydrodynamic (EHL) and eventually hydrodynamic (HD) lubrication regimes, the oil phase (HOSO) facilitated entrainment of a fluid film. This behavior likely results from the formation of a crystal network matrix (Fig. 1a-b), which exhibits dominant elastic behavior ($G' > G''$), as demonstrated in our previous work (Tenorio-Garcia et al., 2023). This minimizes direct surface contact, enhances load distribution resistance, and facilitates the formation of a thin lubricant layer across the surface. This is not surprising and closely aligns with previous research about the role of solid fat content (SFC) in both pure and mixed oils, showing reduced μ values, particularly at low speeds (Tecuanhuey et al., 2024). Previous studies on W/O simple emulsions stabilized solely by surfactants have shown a dependence on water content, with significant frictional forces recorded at higher water concentrations (Douaire et al., 2014). However, in our case, μ values decreased when water content reached 60 v/v% (Fig. 3a). We hypothesize that the structure provided by the CBolg significantly influences the tribological performance of the emulsions, making it largely independent of the added water content within the experimental window tested in this study.

In the same study, Douaire et al. (2014) also reported that higher viscosity in surfactant-stabilized W/O emulsions correlated with increased μ values in the hydrodynamic regime, with a notable increase observed for systems containing 60 % v/v water. However, unlike those findings, W/O single emulsions stabilized with CBolg (Fig. 3a) demonstrated frictional behavior that remained largely independent of water content up to 50 v/v%. This aligns with results reported by Benner et al. (2005), who observed that film thickness in surfactant systems was almost independent of water concentration and particle size, albeit with emulsions with water contents up to 30 v/v% and different tribological conditions.

3.1.2. *Biomimetic tongue-like surface*

The surface characteristics of tribopairs influence the frictional behavior of food systems, as evidenced by tribological measurements conducted using a soft, textured, 3D biomimetic, tongue-like surface (Andablo-Reyes et al., 2020; Soltanahmadi, et al., 2022, 2023). As shown in Fig. 3b, the μ values differ notably between the HOSO, CBolg, and the W/O emulsions highlighting the importance of tongue surface properties (*e.g.* topography). Results indicate that structured systems, such as CBolg and W/O emulsions with 30 % and 50 % v/v water, exhibited comparable μ values in the boundary regime (speeds $<10^{-4}$ m/s) which were lower than those of HOSO. This demonstrated the effective fat-driven lubricity of CB where contacting surfaces are at close proximity. However, an increase in μ values in EHL and HD regimes for CBolg was evident compared to HOSO, suggesting interference of solid crystals in fluid film lubrication.

The presence of water (*i.e.* emulsions) and its concentration influenced the μ values at low-speeds (10^{-4} m/s) and more pronounced effect observed in the EHL and HD regimes. A higher water content appeared to increase μ values in EHL and HD regimes which was likely induced by particle effects associated with dispersed water droplets (Soltanahmadi et al., 2023). Further, at higher water concentration (50 % and 60 %) the transition from the mixed to the EHL regime occurs at lower speed values with higher μ values in the EHL regime which can be attributed to higher viscosity of those samples (Fig. S1) and higher number of water droplets, respectively. At this defined value of entrainment speed, a fluid with greater viscosity generates greater hydrodynamic forces leading to higher μ values in the EHL and HD regimes. Further, greater hydrodynamic forces enhance fluid film formation, therefore, accelerating the transition to EHL and HD regimes (Sarkar et al., 2021). This interpretation is supported by the microstructural observations (Fig. 4a) and the droplet count analysis (Fig. 4c–d), where the 60 % emulsion exhibited a peak of approximately 700 droplets in the size distribution, compared to a maximum of around 200 droplets for the 50 % emulsion.

Analysis of the droplet distribution size via confocal microscopy (Fig. 4b–d) and machine learning (ML) -based image analysis revealed a broad size distribution, ranging from 0.2 µm to 170 µm in Feret diameter. As water content increased, a higher proportion of smaller droplets (<10 µm) was observed, along with the formation of smaller proportion

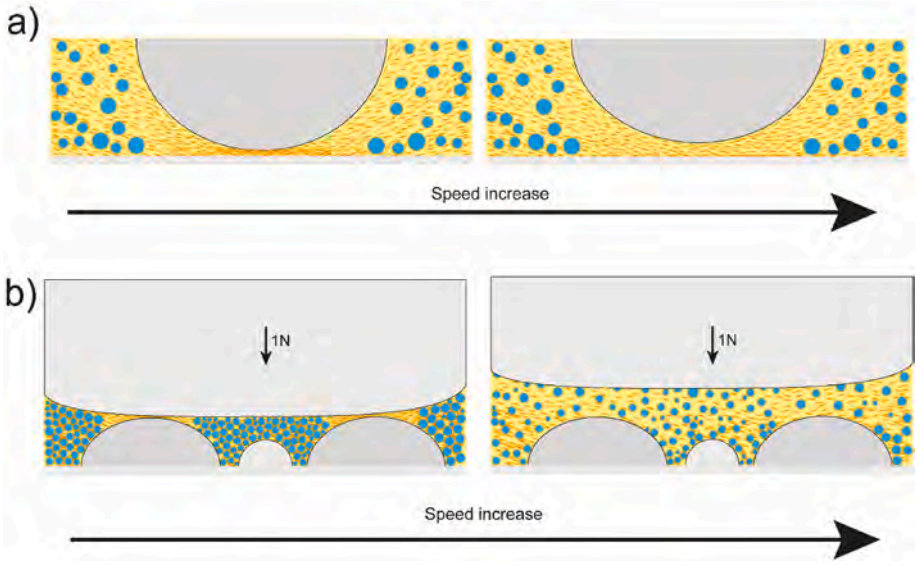

Fig. 5. Schematic illustration of the proposed lubrication mechanism studied using the (**a**) smooth, hydrophobic, PDMS surface and soft, textured, biomimetic tongue-like surface (**b**), in presence of W/O emulsions at 21 °C.

of larger droplets. In emulsions with 50 and 60 % v/v water, droplet sizes exceeding 100 μm were detected, whereas the largest droplets in the 30 % v/v water emulsion measured only 60 μm. The D50 and D90 parameters were used to assess changes in droplet size distribution before and after the tribological test (Fig. 4e). Despite the presence of larger droplets at higher water concentrations, smaller droplets dominated the emulsion structure, as reflected in the D90 values: 2.86 ± 0.48 μm for the 30 % v/v water emulsion compared to 3.1 ± 0.18 μm for higher water content (*i.e.* 60 % v/v).

Furthermore, the high elastic modulus (G′) values (close to 10^3 Pa) previously reported (Tenorio-Garcia et al., 2023) in the same system revealed that adjacent droplets form a structural network, contributing to the emulsion's self-supported elastic structure where droplets act as "active fillers" (Du et al., 2024; Tenorio-Garcia et al., 2023). This structural integrity likely explains the increased μ values in the EHL and HD regimes, as smaller droplets not only fit into the gaps between biomimetic tongue papillae but also behave as part of a larger structured entity, potentially enhancing the surface separation (thicker fluid film) or hindering oil entrainment and consequently affecting lubrication as illustrated in the schematic diagram (Fig. 5b).

Previous research on hard surfaces reported that water is expelled from the emulsion before entering the contact region, rendering water fraction and the droplet size irrelevant to tribology behavior (Benner et al., 2005). However, our results demonstrate that increasing water content reduces the sliding speed required to achieve EHL, aligning with findings from studies conducted on soft surfaces (Douaire et al., 2014). This suggests that small water droplets may be entrained within the contact zone of weakly polar biomimetic tongue-like surface similar to what can be potentially happening in the mouth, possibly due to the high viscosity and consequently high drag forces of the emulsions.

The behavior of the 30 % v/v W/O emulsion (Fig. 4b), which closely resembles that of CBolg, suggesting minimal influence of water droplets in tribological context. This results in the emulsions behaving more like pure oil (HOSO), as supported by the observed lower G' values for 30 % v/v W/O emulsions compared to emulsions with higher water content. Microstructural analysis of the 30 % v/v W/O emulsions (using ML) after tribology further revealed significant coalescence, with a notable reduction in smaller droplets and an increase in droplets size ranging from 4 to 15 μm, yet droplets exceeding 100 μm was not observed (Fig. 5b). The D50 and D90 values are in line with the distribution observation as both values decreased notably after test, indicating potential coalescence or growth of medium and large droplets. This change in droplet size appears to be less important for tribology performance, as it behaves similar to CBolg. In contrast, at higher water fractions, the tribological behavior of the emulsions also exhibited dependence on water concentration, related whit the stronger droplet-matrix interactions that lead to a more robust network of water droplets. For instance, the 50 % v/v, W/O emulsions showed no significant difference or signs of major instability in the droplet size distribution post-tribology testing (named as TT), apart from a slight increase in droplet size and the emergence of two further size bins above 100 μm (Fig. 4c). This suggests that the 50 % v/v W/O emulsions exhibit greater structural stability during tribological testing or pointing to droplet break-up as suggest by the decrease in the D50 and D90 values, especially for medium droplets (D90) as can be seen in Fig. 4e. Additionally, at higher sliding speeds shifting the lubrication regime to HD, the influence of water concentration on tribological performance appears to come from the greater force required to move more structured systems, due to higher viscosity values.

Emulsions with higher water content (60 % v/v water) demonstrated stable microstructure under static conditions for up to seven months (Tenorio-Garcia et al., 2023). However, during tribological testing, their performance was irregular, likely due to compromised stability under shear conditions (Fig. 3b). Although the 60 % v/v W/O emulsions initially contain a high concentration of small water droplets, larger droplets were also present, and further coalescence occurs during tribotesting, leading to increased droplet size as there is an increase in droplet size between 1 and 5 μm and 100 μm (Fig. 4d). This instability may be attributed to relatively lower free CB crystals per volume unit of water, which is insufficient to form a stable network under tribological shear which exacerbates instability (Fig. 1a–b); thereby limiting the emulsion's structural integrity under dynamic frictional forces. These results emphasize the critical role of droplet packing and network dynamics in influencing tribological performance, particularly at higher water contents.

Based on these findings, it can be inferred that adding up to 50 % v/v water may not adversely affect the perception at low sliding speeds, which is favorable for replicating creaminess — a sensory attribute crucial to oily food products that becomes perceptible at low sliding speeds (Corvera-Paredes et al., 2022). However, the 30 % v/v water W/O emulsion is the only emulsion to exhibit behavior almost similar to that of the pure CBolg, suggesting that a water content of 30 % could be the upper limit before differences in sensory perception arise, however such data would need sensorial validation. To summarize, Fig. 5

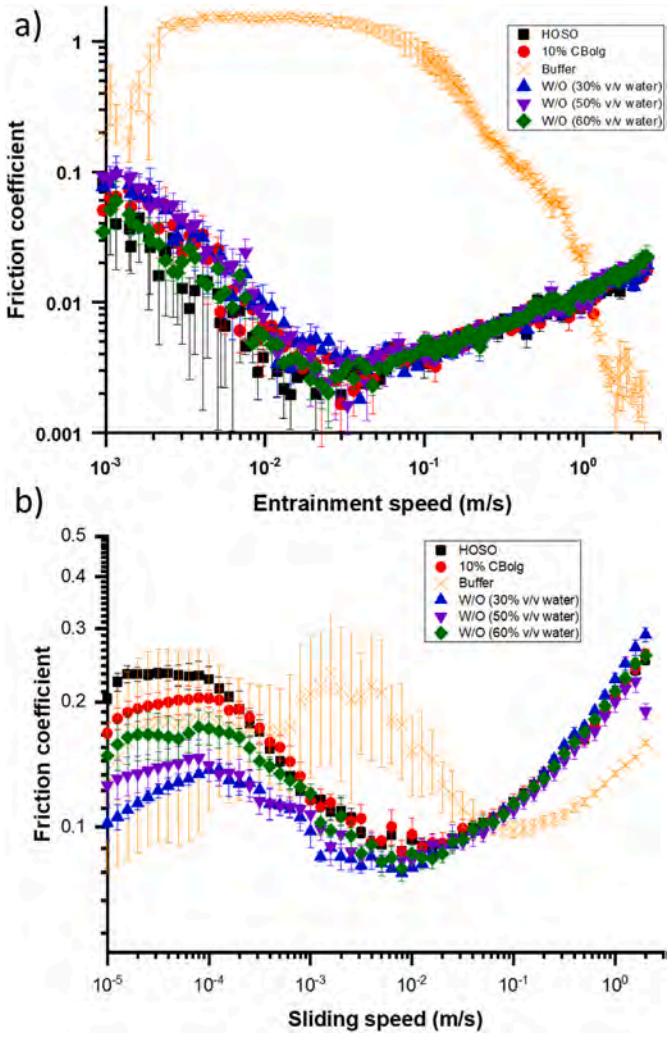

Fig. 6. Friction coefficient (μ) versus entrainment speed in smooth, hydrophobic polydimethylsiloxane (PDMS) contact surface (**a**) and sliding speed in textured, soft, biomimetic tongue-like surface (**b**), respectively, for high oleic sunflower oil, 10 % v/v CB oleogel (CBolg), 10 mM phosphate buffer (Buffer), and W/O emulsions with varying water concentrations (30 % v/v, 40 % v/v, 50 % v/v, and 60 % v/v water). Measurements were conducted at 37 °C.

illustrates the configurations and the lubrication mechanisms of the MTM setup (Fig. 3a), and biomimetic tongue surface set up (Fig. 5b). On PDMS surfaces, a thin oil layer forms effectively. The crystal network of the oleogel provides structural support, limiting the interaction between surfaces at the contact point and resulting in lower μ values. In this configuration, water does not play a significant role, as evidenced by its negligible contribution to the observed μ values (Fig. 5a). In contrast, the distribution of the bumps, simulating the papillae configuration of a human tongue, may serve as micro-reservoirs for lubricant contributing to the reported friction at lower speeds, $<10^{-4}$ m/s (Fig. 5b). The internal structure offered by the fat crystals provides superior mechanical support compared to pure oil (Fig. 5b). At higher speeds, a thicker film forms including small water droplets which contributed to the increase in the μ values at higher water ratio. This setup enables discrimination between emulsions with different water content, with increased sensitivity to higher concentrations.

3.1.3. Effect of temperature on the W/O emulsions for both tribological surfaces

Measurements at 37 °C provide insights into the tribological behavior of the system at temperatures close to the oral conditions. Tribology results obtained using the smooth, hydrophobic, PDMS tribopairs (Fig. 6a) revealed that both CBolg and the W/O emulsions, regardless of water concentration, exhibited comparable performance to HOSO throughout the speed range, indicating a predominant oil-like behavior. These findings suggest that the oleogel and the CB-stabilized emulsion structures melt at this temperature, confirming the critical role played by the fat crystal network in solid state in determining tribology behavior. At 37 °C, the fat crystals are fully molten, as previously observed on similar systems (Metilli et al., 2021; Tenorio-Garcia et al., 2023).

In contrast, results obtained using a biomimetic tongue surface (Fig. 6b) showed notable differences at lower sliding speeds ($<10^{-3}$ m/s) what appears to be mixed and boundary remiges, particularly for structured systems like emulsions. For instance, the CBolg exhibited friction (μ = 0.20) comparable to HOSO (μ = 0.23) in the boundary regime. Additionally, these crystals either melt or lose their structural influence during the test, resulting in a primarily oil-like behavior for CBolg in both EHL and hydrodynamic regimes. The emulsions consistently showed lower μ values compared to the CBolg, with lower μ values at lower water concentration. For example, at 30 % v/v water

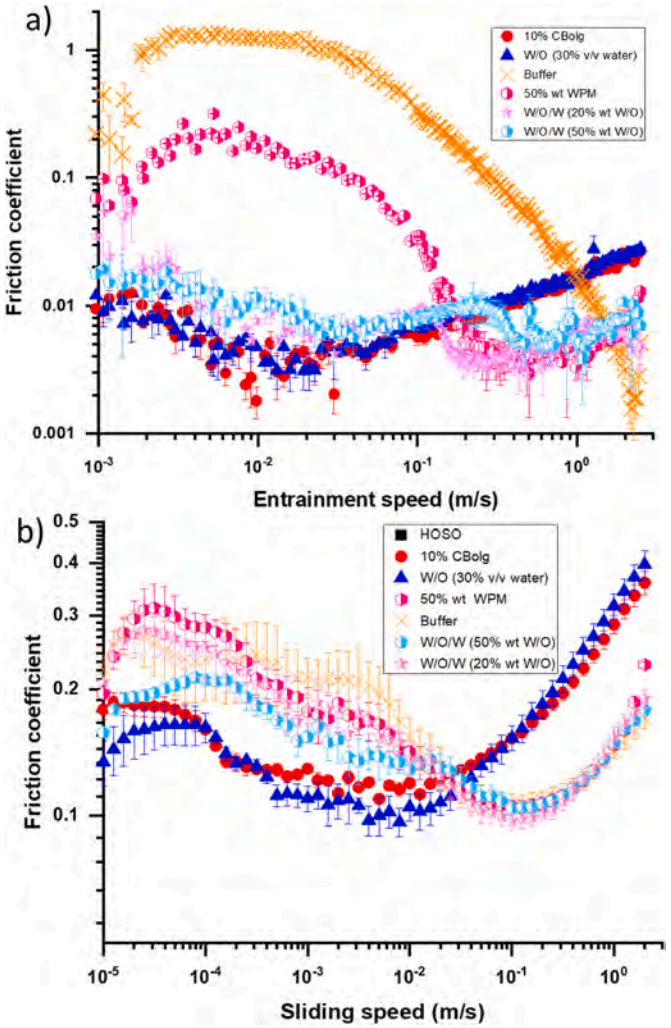

Fig. 7. Friction coefficient (μ) versus entrainment speed in smooth, hydrophobic polydimethylsiloxane (PDMS) contact surface (**a**) and sliding speed in textured, soft, biomimetic tongue-like surface (**b**), respectively, for 10 % v/v CB oleogel (CBolg), 30 % v/v W/O emulsions, 10 mM phosphate buffer (Buffer), 50 % w/w whey protein microgel (WPM), and W/O/W DEs with varying water concentrations (20 % wt and 50 % wt W/O emulsion). Measurements were conducted at 21 °C.

content, the μ value was 0.12 at a speed of 5×10^{-5} m/s, whereas at 60 % v/v water content, it slightly increased to 0.16. The reason for such observation is not clear but it was probably influenced by the breakdown of the emulsion structure causing phase separation and hence affecting physicochemical properties of the system such as viscosity and surface adsorption. Further studies are required to better understand this transition.

Despite these variations, all systems transitioned to an oil-like behavior at speeds $>10^{-3}$ m/s. This observation suggests that, regardless of water concentration, the film thickness at these speeds is predominantly governed by the oil phase, when the structure is lost due to melting of CBolg. These findings align with previous results on hard surfaces (Benner et al., 2005), where the tribological behavior was independent of water concentration (in the absence of particles). This further highlights the role of dispersed lubricating fat particles (CBOlg here) in enhancing lubrication performance within structured systems particularly at temperatures where the particle-laden interfaces are still intact unlike at physiological temperatures, where largely it is a fat-driven phenomena regardless of water content.

3.2. Soft tribology of the dual Pickering W/O/W double emulsions (DEs)

3.2.1. Smooth hydrophobic surface

DEs exhibit a more complex structure compared to single W/O emulsions. Within each oil droplets, there are numerous smaller water droplets, forming a multi-compartmentalized system (Fig. 1c and d). When DEs are stabilized using a dual Pickering-stabilized approach, the complexity increases further, as the oil phase not only contains water droplets but also incorporates solid crystals. This crystal network might provide additional rigidity and stability to the oil droplets, which could potentially influence the tribological performance of the system. In addition, microgels (WPM) may contribute to lubrication by stabilizing the oil droplets (in this case DEs) at the interface or through the presence of unabsorbed microgels, both of which have demonstrated lubrication performance (Andablo-Reyes et al., 2019; Kew et al., 2023; Soltanahmadi et al., 2022; You, et al., 2023, 2024). By building upon the aforementioned findings from the W/O emulsions stabilized with CB crystals, this section examines the lubrication behavior of double emulsions.

The tribology of PDMS surfaces in presence of DEs revealed that structured DE systems exhibited superior lubrication compared to the WPM dispersion ($p < 0.05$) at $< 10^{-1}$ and similar lubrication behavior to W/O and CBolg ($p > 0.05$). (Fig. 7a). However, at speeds >0.3 m/s for 50DE (containing 50 % wt W/O) and >0.2 m/s for 20DE (containing 20 % wt W/O), a clear transition towards WPM-driven lubricity was observed for DEs where they collapsed in the HD lubrication regime. This inner droplet (W/O) concentration–dependent transition can be attributed to shift from oil-driven lubricity (through oil droplet coalescence in DE) to water-mediated lubricity in the HD regime (Fig. 7a). This transition from oil to water mediated lubrication may influence oral perception. At low speeds, the lower μ values observed for DEs could be associated with creaminess sensations. Such associations between friction and sensory attributes have been previously described in oil-continuous systems, such as Milk (Liu et al., 2016). In contrast, the shift towards water-driven lubrication at higher speeds may help reduce thickness, as suggested by the lower μ values observed for DEs compared to W/O and CBolg in the HD regime. Previous research has shown that microgel-based systems can enhance lubricity (Andablo-Reyes et al., 2019; Pabois et al., 2023). In addition, a positive correlation between viscosity and sensory perception of thickness has been reported for hydrocolloid-thickened systems such as starch and xanthan gum (Sharma et al., 2022). In our study, DEs exhibited lower viscosity (Fig. S1) than oil-based systems (*e.g.*, CBolg and CBolg-based W/O emulsions), which explain the lower friction values observed in the HD regime. This regime, characterized by high entrainment speeds, is dominated by the bulk viscosity of the lubricant rather than surface interactions. Consequently, the reduced viscosity of DEs could be associated with lower perception of thickness and a less coating or adhesive mouthfeel. This suggest that both the softness of the WPM lubrication contribute synergistically to the enhanced oral lubricity and cleaner mouthfeel of DEs.

Previous studies have reported that water droplets within the DE droplets tend to form larger structures that are more resistant to deformation, thereby reducing the likelihood of DEs droplets entering the contact area (M. Chen, Li, et al., 2022; Oppermann et al., 2017). Additionally, research has shown that DEs exhibit lower μ values compared to simple O/W emulsions. This has been attributed to the presence of other components, such as polyglycerol polyricinoleate (PGPR), which forms micelles in the outer aqueous phase and influences tribological performance more significantly than the DE droplets themselves, particularly when the droplets are relatively large (*e.g.*, 50 μm) (Oppermann et al., 2017). However, no surfactants were added in this study. Instead, the observed behavior is likely linked to the droplet size distribution. Although the DE droplets were relatively larger ($D_{[4,3]} = 75.5\ \mu m \pm 1.5$), which would make their entrapment in the contact area challenging, a subpopulation of smaller droplets (<1 μm; Fig. S2) may contribute to the initial oil-like lubrication, most possibly these comes from the simple emulsion that have not been emulsified into DE in the homogenization process.

Previous research on the effect of the droplet size distribution in O/W emulsions found that larger droplets (≈4 μm) provide better lubrication than smaller (≈0.3 μm) due to their ability to deform, squeeze, and entrain into the lubricant gap, subsequently coalescing and supporting film formation (Q. Wang, Zhu, Ji, & Chen, 2021). In the droplet size distribution of the studied dual Pickering-stabilized DEs, a distinct peak was observed for droplets ranging from 3 to 19 μm. These smaller droplets could coalesce under shear, providing lubrication similar to that of oil-continuous systems. However, this effect appears to be dependent of the sliding speed, as the system transitions through the observed shift in lubrication behavior. Beyond this shift, lubrication becomes entirely dominated by the continuous phase, in this case, the WPM dispersion (Fig. 7a). This is not surprising as deformable sub-micron sized *free* microgels in the continuous phase can get entrained unlike the large DEs and provide lubrication as observed in previous studies, but not in the context of DEs. To our knowledge, we are the first to report that the DEs are behaving like WPM dispersions, this is largely attributed to size effects in the smooth tribopair conditions as illustrated schematically in Fig. 9a.

3.2.2. Biomimetic tongue surface

Contrary to the behavior observed in the smooth, PDMS tribopair setup, DEs in the biomimetic setup, irrespective of speed, did not exhibit lubrication properties similar to oil-systems especially at low droplet concertation (*i.e.* 20 % W/O droplets) (Fig. 7b). Instead, their behavior aligned more closely with that of the WPM dispersion. The deviation of the lubrication performance of DE from the WPM system was greater at higher W/O concentration which approached towards the lubrication behavior of CBolg. The transition to the mixed regime occurred at slightly lower μ values for the 20DEs (i.e. containing 20 wt% W/O emusions), with minor differences observed at sliding speeds below 0.0003 m/s. Beyond this point, both systems displayed similar behavior, reaching the EHL regime at higher speeds compared to the oil systems. This indicates a reduced capability to form the minimum film thickness required to fully separate the surfaces.

The concentration of the inner droplets (W/O emulsions) in the DEs also influenced their behavior at low speed (10^{-5} m/s). The DEs containing 50 % W/O (50DEs) exhibited lower μ value (0.15) compared to 20DEs (0.20). This difference diminished as the friction value for 50DEs increased, eventually converging with the WPM and 20DE curves. The transition to the mixed regime occurred slightly late for the 50DE tribological behavior, though its tribological behavior matched the WPM and 20DEs at a sliding speed of 0.012 m/s. This suggests that

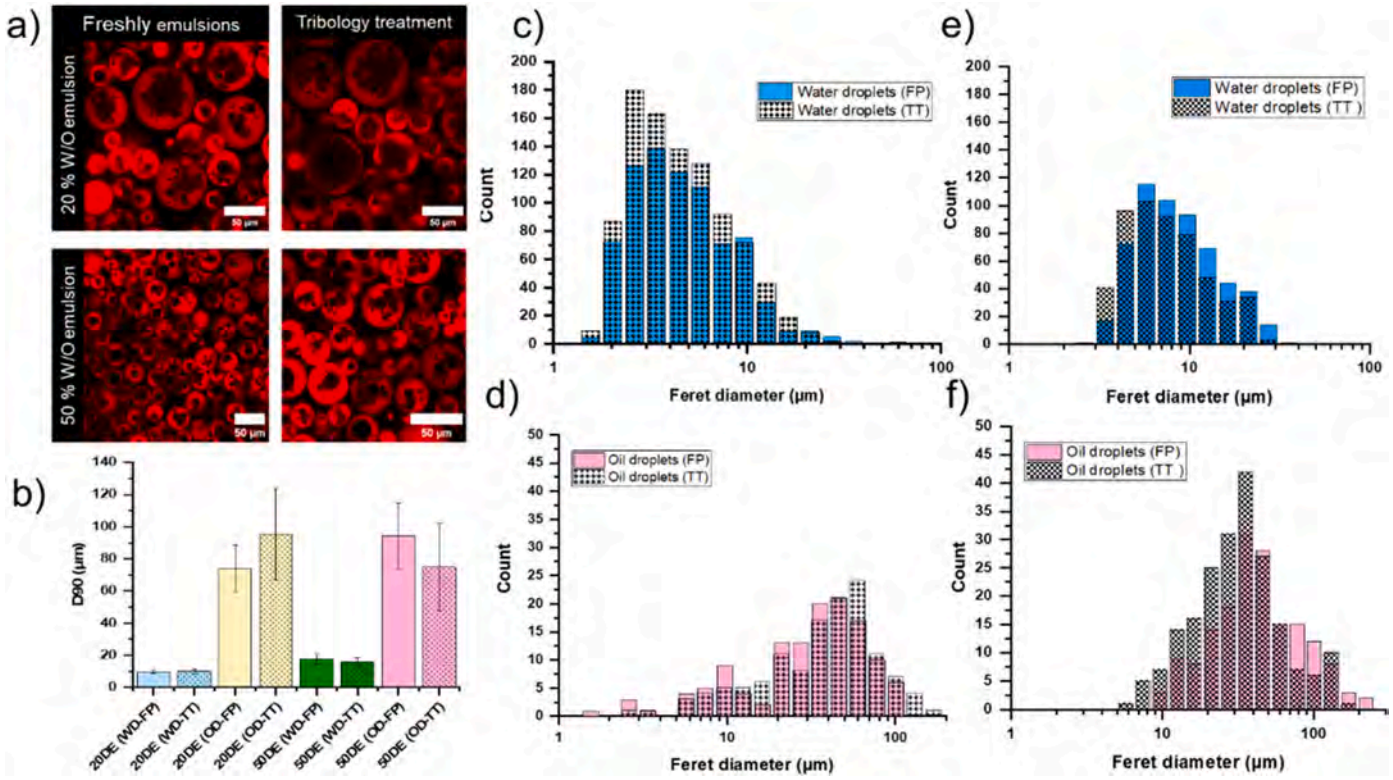

Fig. 8. Morphological evolution of W/O/W DEs before and after exposure to frictional forces in a biomimetic tongue-like surface at 21 °C. Microstructural changes in W/O/W emulsions with 20 % (20DE), 50 % (DE50) W/O emulsions concentration (**a**). D90 of 20DE and 50DE emulsions before and after tribology test are shown in **b**. Droplet size distribution changes for internal water droplets (**c** and **d**) and the external oil droplets (**e** and **f**) for both 20DE (**c**–**d**) and 50DE (**e**–**f**). FP stands for the freshly prepared emulsions, while TT stands for post-tribology test.

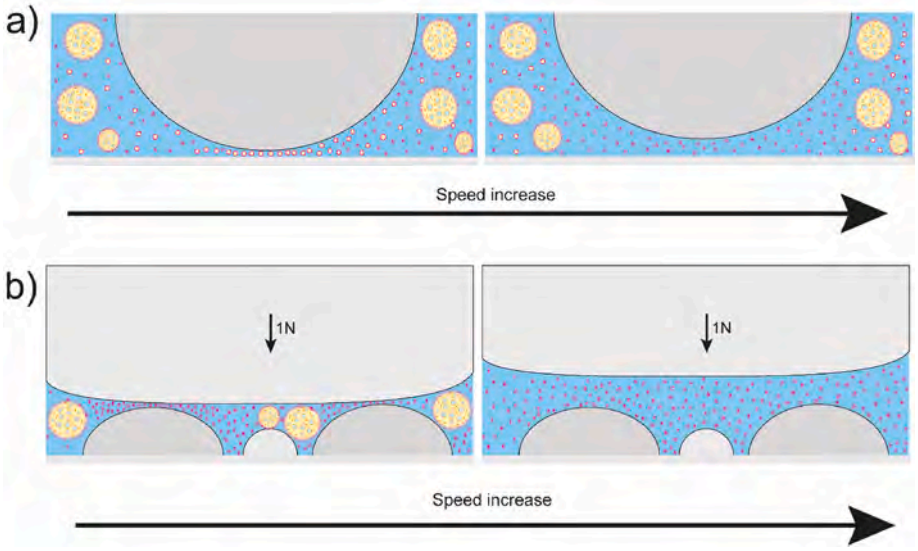

Fig. 9. Schematic illustration of the proposed lubrication mechanism studied using the (**a**) smooth, hydrophobic, PDMS surface and (**b**) soft, textured, biomimetic tongue-like surface, in presence of W/O/W emulsions at 21 °C.

microgels predominantly govern the tribological behavior at higher speeds. The reduced initial μ value for the 50DEs could be associated with a greater number of droplets potentially trapped in the gaps between the fungiform and filiform shaped papillae on the biomimetic tongue, and probably to the collapse of the film formed by the small and limited oil droplets that as speed increase could not form a film (Cambiella et al., 2006).

Fig. 8 illustrates the microstructure before and after tribological testing using the biomimetic tongue-like surface (Fig. 8a), along with the internal (water) and external (oil) droplets size distributions for the 20DEs and 50DEs (Fig. 8c–f). The results show minimal structural changes in the DEs after frictional forces were applied. A minor new peak was observed in the inner water droplets size distribution at approximately 70 μm (Fig. 8c), while two small peaks emerged in the external oil droplets distribution above 100 μm (Fig. 8d) for 20DEs. However, these changes were not statistically significant. These findings

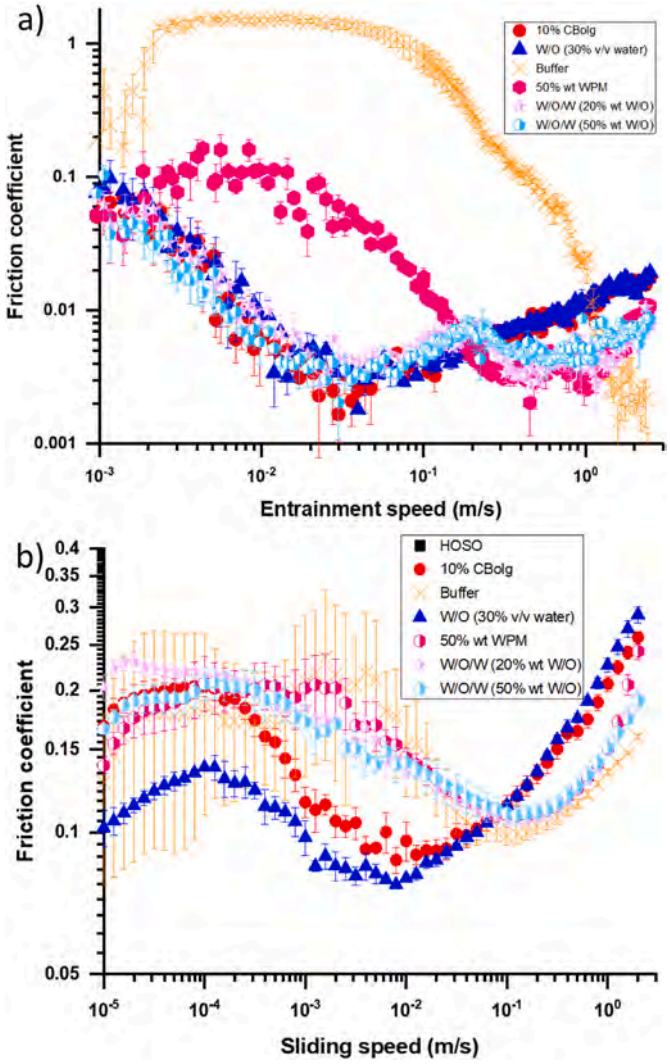

Fig. 10. Friction coefficient (μ) versus entrainment speed in smooth, hydrophobic polydimethylsiloxane (PDMS) contact surface (**a**) and sliding speed in textured, soft, biomimetic tongue-like surface (**b**), respectively, for 10 % v/v CB oleogel (CBolg), 30 % v/v W/O emulsions, 10 mM phosphate buffer (Buffer), 50 % w/w whey protein microgel (WPM), and W/O/W DEs with varying water concentrations (20 % wt and 50 % wt W/O emulsion). Measurements were conducted at 37 °C.

support the hypothesis that larges droplet sizes and its low deformability prevent the droplets from entering the contact area. Consequently, the microgel structure becomes more relevant to the observed tribological behavior. Additionally, the hydrophilic nature of the biomimetic tongue surface may preferentially interact with the aqueous phase (Andablo-Reyes et al., 2020)(Soltanahmadi et al., 2023), especially when oil droplets are large and minimally deformed. This interaction likely results in lubrication dominated by water and microgel structures within the contact area.

For the 50DEs, the droplet size distribution (Fig. 8e–f) also displayed no significant changes. Interestingly, the D90 values (Fig. 8b) for the oil droplets in 50DEs decreased, suggesting that smaller droplets may have deformed or broken at high speeds, hence better lubricity at low-speed values. In contrast, the 20DE exhibited an increased tendency towards coalescence of oil droplets. Despite these observations, the oil droplets in the DEs do not appear to play a significant role in the tribological behavior. Such findings could not have been achieved without ML-assisted image analysis of inner droplets where it is challenging to achieve droplet sizing results using light scattering experiments.

In DE systems, the higher viscosity of the oil droplets, influenced by their internal water content and crystalline network, reduces their likelihood of deformation. At higher W/O ratio, the oil droplets can initially be accommodated in the gaps between the fungiform and filiform structures (droplet size < height of fungiform/filiform) in larger numbers and therefore, may either a) increase the contact area in the biomimetic tongue system, or b) provide a localized separation between contacting surfaces to allow interposition of the fluid film between the surfaces. In both scenarios the resistance to deformation lead to a temporary lifting effect contributing to the lower μ values observed at $u < 10^{-3}$ m/s. At $u > 10^{-3}$ m/s the effective lubricant is the WPM solution, and the W/O droplets do not appear to play a role probably due to their rigidity and large size and making their movement across the surface challenging. Fig. 9b depicts this proposed lubrication mechanism. It is also crucial to acknowledge the uncertainty regarding the number of fungiform structures in contact with the glass ball. Future work will be necessary to experimentally observe the microstructure-surface interactions on behavior of single and double emulsions using an *in situ* optical-tribology set-up (Soltanahmadi et al., 2023).

3.2.3. *Effect of temperature on DEs for both tribological surfaces*

When the DEs were subjected to tribological shear at 37 °C, the μ values increased by an order of magnitude at the initial speed (10^{-3}), from approximately 0.01 to nearly 0.1 (Fig. 10a) in smooth PDMS surface. Regardless of the W/O concentration, the DEs exhibited mixed and hydrodynamic lubrication regimes, similar to those observed for CBolg and W/O emulsions. As previously noted, the CB crystals melt at this temperature, destabilizing the inner water droplets. This instability leads to coalescence and subsequent diffusion of the internal water phase into the external phase, as shown in the confocal microscopy images Fig. 11.

The loss of the internal structure resulted in collapse of friction graphs of DEs into those of CBolg and W/O emulsions confirming the crucial role of internal structure of the DEs on their lubrication properties (Fig. 10a). While larger droplets might not directly contribute to the contact area, smaller oil droplets containing less water or primarily CB crystals dispersed in the oil phase likely form an initial lubricating layer. This layer mimics oil-based systems by developing a sufficient film thickness to separate surfaces in the EHL regime. However, as temperature increases, the structure, particularly that formed by CB crystals, breaks down, resulting in lubrication behavior more typical of oil-dominated systems. Despite these observations, it remains unclear whether the tribological response of the DEs arises from simple O/W emulsions formed during the secondary homogenization step, or from small oil droplets that still encapsulate water and CB crystals and are small enough to participate in the contact area.

Research on diluted O/W systems on metal surfaces has demonstrated that an EHL regime representative of oil-lubricated contact can be achieved even with diluted emulsions. However, this film thickness can collapse due to starvation, as the amount of oil supplied to the contact is insufficient for the film thickness to increase with the speed (Cambiella et al., 2006). A similar phenomenon is evident also in the DEs at 37 °C, suggesting that larger droplets do not significant influence tribological performance. Once the film collapses, the DEs behave similarly to the WPM solution.

Conversely, in the biomimetic tongue system, no significant differences were detected between the emulsions and the WPM dispersions, even for the 50DEs at 37 °C (Fig. 10b), which exhibited comparable tribological behavior to WPM solution, despite the coalescent observed (Fig. 11). Although a slight increase in μ was observed for the 50DEs at low speeds, the system ultimately behaved like the WPM dispersion. This indicates that the internal structure of the DEs contributes to lower the μ values for higher O/W concentration in the DEs; however, once the structure is disrupted, no differences are observed. In summary, this suggests that sub-micron-sized microgels might drive the lubrication phenomena when the droplets themselves cannot enter the contact

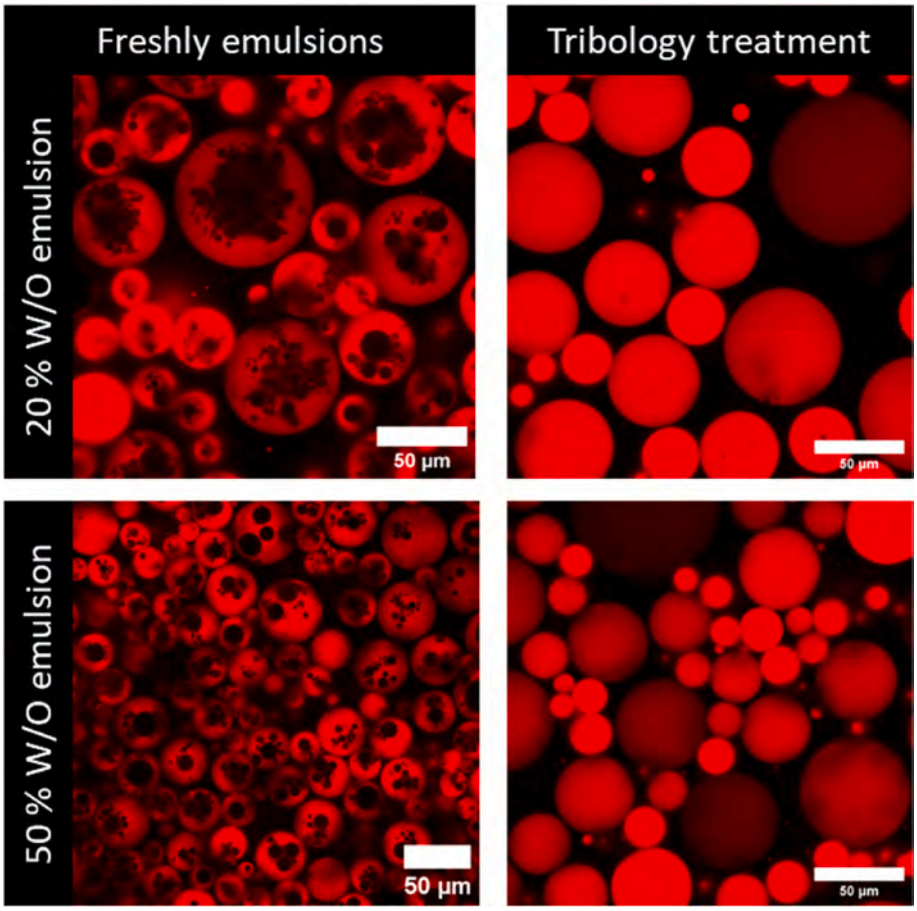

Fig. 11. Microstructural changes in DE with 20 % and 50 % (w/w) W/O emulsion concentration after exposure to frictional forces in a biomimetic tongue-like surface at 37 °C.

because of their larger dimensions.

4. Conclusions

This study demonstrated the dominant role of the cocoa butter oleogel-based crystals in governing the tribological behavior of Pickering water-in-oil and dual water-in-oil-in-water Pickering double emulsions. The tribological results displayed significant variations depending on the smooth versus textured biomimetic tongue-like surface. The smooth surface results demonstrate that emulsions stabilized solely by the oleogel crystals showed superior lubrication properties, with friction coefficient values significantly lower at low speeds. The oleogel network's ability to maintain a lubricating oil film contributes to low friction coefficients. The addition of water to the structured oleogels does not significantly affect the tribological properties, maintaining a lubrication regime that is largely independent of the water concentration. However, in the biomimetic tongue surface, the tribological measurements reveal a clear dependence on water content, with emulsions having higher water concentrations, exhibiting lower friction coefficient values in the boundary regime, largely attributed to the elasticity of the water-in-oil emulsion system acting a continuous fat-like fluid film entrained in the contact area. Additionally, the droplet size distribution (supported by ML analysis) influenced the tribological behavior, with smaller droplets fitting into the gaps of the tongue papillae, which reduced the friction. These findings indicate that the structured crystal network in the emulsions significantly contributes to lubrication efficiency, with water content and droplet size distribution playing key roles in tribological behavior.

Despite the effect of water on friction coefficients in the boundary and mixed regime, it is unlikely that the water droplets enter the contact area in these regimes. Therefore, friction coefficients are dominated by the structure provided by the oleogel crystals, as all of them presented friction values close to the oleogels until the flow motion get close to the electrohydrodynamic lubrication regime. The size of fat crystals is in the order of nanometer, which means they could interpose in between contact bodies. However, the reduction of friction, at speeds $<10^{-4}$ m/s, is associated with the water droplets providing structural reinforcement (provided by high G') that increase contact area, but the shear thinning behavior finally enables the system to become more similar to the CBolg for the hydrodynamic regime.

In double emulsions on the other hand, the presence of structured oil droplets and an internal crystal network significantly influenced the lubrication regime, facilitating earlier transitions to the elastohydrodynamic regime with higher oil content. The tribological performance varies with both oil concentration and droplet size distribution. The effect of temperature, particularly at 37 °C destabilizes the internal structure of water droplests within the double emulsion due to melting of the oleogel crystals, leading to increased friction highlighting the relevance of the structure in the system. In the biomimetic tongue surface system, double emulsions did not demonstrate oil-like lubrication but rather behaved similarly to water-based systems, largely dominated by the microgel particles in the continuous phase.

These findings suggest that the combination of emulsions characteristics (*e.g.*, droplet size, internal structure, elasticity, viscosity) may influence the tribological performance, latter also influenced by the topography (*e.g.,* fungiform, and filiform shapes), contact pressure (PDMS *vs* the elastomer in biometric tongue) and chemistry of the surfaces used (wettability). Further validation through sensory testing is

essential to establish a direct correlation between frictional measurements and perceived creaminess.

CRediT authorship contribution statement

Elizabeth Tenorio-Garcia: Writing – review & editing, Writing – original draft, Visualization, Methodology, Investigation, Funding acquisition, Data curation, Conceptualization. **Siavash Soltanahmadi:** Writing – review & editing, Methodology, Data curation, Conceptualization. **Jens Saalbrink:** Writing – review & editing, Methodology, Formal analysis, Data curation, Conceptualization. **Jose C. Bonilla:** Writing – review & editing, Project administration, Methodology, Conceptualization. **Michael Rappolt:** Writing – review & editing, Supervision. **Elena Simone:** Writing – review & editing, Supervision. **Anwesha Sarkar:** Writing – review & editing, Supervision, Project administration, Methodology, Conceptualization.

Declaration of competing interest

No conflicts of interests.

Acknowledgements

ET-G acknowledges financial support from the Mexican National Council of Science and Technology (CONACyT) for the award of an Academic Scholarship for her PhD studies. ES has received funding for this collaboration from the European Research Council (ERC) under the European Union's Horizon 2020 research and innovation program (grant agreement No 949229). AS acknowledges the funding from British Council ISPF Grant (47652866).

Appendix A. Supplementary data

Supplementary data to this article can be found online at https://doi.org/10.1016/j.foodhyd.2025.112035.

Data availability

Data will be made available on request.

References

Andablo-Reyes, E., Bryant, M., Neville, A., Hyde, P., Sarkar, R., Francis, M., & Sarkar, A. (2020). 3D biomimetic tongue-emulating surfaces for tribological applications. *ACS Applied Materials & Interfaces, 12*(44), 49371–49385.

Andablo-Reyes, E., Yerani, D., Fu, M., Liamas, E., Connell, S., Torres, O., & Sarkar, A. (2019). Microgels as viscosity modifiers influence lubrication performance of continuum. *Soft Matter, 15*(47), 9614–9624.

Araiza-Calahorra, A., Mackie, A. R., & Sarkar, A. (2024). Oral tribology of dairy protein-rich emulsions and emulsion-filled gels affected by colloidal processing and composition. *Current Research in Food Science, 9*, Article 100806.

Ares, G., & Varela, P. (2017). Trained vs. consumer panels for analytical testing: Fueling a long lasting debate in the field. *Food Quality and Preference, 61*, 79–86.

Bao, Y., Liu, K., Zheng, Q., Yao, L., & Xu, Y. (2021). A review of preparation and tribological applications of Pickering emulsion. *Journal of Tribology, 144*(1).

Benner, J. J., Sadeghi, F., Hoeprich, M. R., & Frank, M. C. (2005). Lubricating properties of water in oil emulsions. *Journal of Tribology, 128*(2), 296–311.

Berg, S., Kutra, D., Kroeger, T., Straehle, C. N., Kausler, B. X., Haubold, C., Schiegg, M., Ales, J., Beier, T., Rudy, M., Eren, K., Cervantes, J. I., Xu, B., Beuttenmueller, F., Wolny, A., Zhang, C., Koethe, U., Hamprecht, F. A., & Kreshuk, A. (2019). Ilastik: Interactive machine learning for (bio)image analysis. *Nature Methods, 16*(12), 1226–1232.

Cambiella, A., Benito, J. M., Pazos, C., Coca, J., Ratoi, M., & Spikes, H. A. (2006). The effect of emulsifier concentration on the lubricating properties of oil-in-water emulsions. *Tribology Letters, 22*(1), 53–65.

Chen, M., Li, W., Wang, W., Cao, Y., Lan, Y., Huang, Q., & Xiao, J. (2022a). Effects of gelation on the stability, tribological properties and time-delayed release profile of double emulsions. *Food Hydrocolloids, 131*, Article 107753.

Chen, J., & Stokes, J. R. (2012). Rheology and tribology: Two distinctive regimes of food texture sensation. *Trends in Food Science & Technology, 25*(1), 4–12.

Chen, M. A., Wang, W., & Xiao, J. (2022b). Regulation effects of beeswax in the intermediate oil phase on the stability, oral sensation and flavor release properties of pickering double emulsions. *Foods, 11*(7), 1039.

Corvera-Paredes, B., Sánchez-Reséndiz, A. I., Medina, D. I., Espiricueta-Candelaria, R. S., Serna-Saldívar, S., & Chuck-Hernández, C. (2022). Soft tribology and its relationship with the sensory perception in dairy products: A review. *Frontiers in Nutrition, 9*, Article 874763.

Douaire, M., Stephenson, T., & Norton, I. T. (2014). Soft tribology of oil-continuous emulsions. *Journal of Food Engineering, 139*, 24–30.

Du, L., & Meng, Z. (2025). Engineering surfactant-free pickering double emulsions gels with different structures as low-calorie fat analogues: Tunable oral perception, inhibiting lipid digestion, and potent co-delivery for lycopene and epigallocatechin gallate. *Food Chemistry, 463*, Article 141378.

Du, L., Zhou, S., Huang, Y., & Meng, Z. (2024). Investigation on the structure characteristics, stability evaluation, and oral tribology of natural oleanolic acid-based water-in-oil high internal phase and multiple pickering emulsions as realistic fat analogues. *Food Chemistry*, Article 142121.

Kew, B., Holmes, M., Liamas, E., Ettelaie, R., Connell, S. D., Dini, D., & Sarkar, A. (2023). Transforming sustainable plant proteins into high performance lubricating microgels. *Nature Communications, 14*(1), 4743.

Kew, B., Holmes, M., Stieger, M., & Sarkar, A. (2020). Review on fat replacement using protein-based microparticulated powders or microgels: A textural perspective. *Trends in Food Science & Technology, 106*, 457–468.

Li, Y., Gong, S., Guan, X., Jiang, H., Tao, S., Yang, C., & Ngai, T. (2021). One-step preparation of all-natural pickering double emulsions stabilized by oppositely charged biopolymer particles. *8*(23), Article 2101568.

Liu, K., Stieger, M., van der Linden, E., & van de Velde, F. (2016). Tribological properties of rice starch in liquid and semi-solid food model systems. *Food Hydrocolloids, 58*, 184–193.

McClements, D. J. (2015). Reduced-fat foods: The complex science of developing diet-based strategies for tackling overweight and obesity. *Advances in Nutrition, 6*(3), 338S–352S.

Metilli, L., Lazidis, A., Francis, M., Marty-Terrade, S., Ray, J., & Simone, E. (2021). The effect of crystallization conditions on the structural properties of oleofoams made of cocoa butter crystals and high oleic sunflower oil. *Crystal Growth & Design, 21*(3), 1562–1575.

Oppermann, A. K. L., Verkaaik, L. C., Stieger, M., & Scholten, E. (2017). Influence of double (w(1)/o/w(2)) emulsion composition on lubrication properties. *Food & Function, 8*(2), 522–532.

Pabois, O., Avila-Sierra, A., Ramaioli, M., Mu, M., Message, Y., You, K.-M., Liamas, E., Kew, B., Durga, K., Doherty, L., & Sarkar, A. (2023). Benchmarking of a microgel-reinforced hydrogel-based aqueous lubricant against commercial saliva substitutes. *Scientific Reports, 13*(1), Article 19833.

Saalbrink, J., Loo, T. Y. J., Mertesdorf, J., Xu, P., Pedersen, M. T., Clausen, M. P., & Bonilla, J. C. (2025). Quantifying microscopic droplets in colloidal systems through machine learning-based image analysis. *Food Hydrocolloids, 166*, Article 111301.

Sarkar, A., Andablo-Reyes, E., Bryant, M., Dowson, D., & Neville, A. (2019). Lubrication of soft oral surfaces. *Current Opinion in Colloid & Interface Science, 39*, 61–75.

Sarkar, A., & Dickinson, E. (2020). Sustainable food-grade Pickering emulsions stabilized by plant-based particles. *Current Opinion in Colloid & Interface Science, 49*, 69–81.

Sarkar, A., Kanti, F., Gulotta, A., Murray, B. S., & Zhang, S. (2017). Aqueous lubrication, structure and rheological properties of Whey protein microgel particles. *Langmuir, 33*(51), 14699–14708.

Sarkar, A., & Krop, E. M. (2019). Marrying oral tribology to sensory perception: A systematic review. *Current Opinion in Food Science, 27*, 64–73.

Sarkar, A., Soltanahmadi, S., Chen, J., & Stokes, J. R. (2021). Oral tribology: Providing insight into oral processing of food colloids. *Food Hydrocolloids, 117*, Article 106635.

Schindelin, J., Arganda-Carreras, I., Frise, E., Kaynig, V., Longair, M., Pietzsch, T., Preibisch, S., Rueden, C., Saalfeld, S., Schmid, B., Tinevez, J.-Y., White, D. J., Hartenstein, V., Eliceiri, K., Tomancak, P., & Cardona, A. (2012). Fiji: An open-source platform for biological-image analysis. *Nature Methods, 9*(7), 676–682.

Sharma, M., Pondicherry, K. S., & Duizer, L. (2022). Understanding relations between rheology, tribology, and sensory perception of modified texture foods. *53*(3), 327–344.

Soltanahmadi, S., Bryant, M., & Sarkar, A. (2023). Insights into the multiscale lubrication mechanism of edible phase change materials. *ACS Applied Materials & Interfaces, 15*(3), 3699–3712.

Soltanahmadi, S., Murray, B. S., & Sarkar, A. (2022). Comparison of oral tribological performance of proteinaceous microgel systems with protein-polysaccharide combinations. *Food Hydrocolloids, 129*, Article 107660.

Spyropoulos, F., Duffus, L. J., Smith, P., & Norton, I. T. (2019). Impact of pickering intervention on the stability of W1/O/W2 double emulsions of relevance to foods. *Langmuir, 35*(47), 15137–15150.

Tecuanhuey, M., Girardi, A., Corrà, L., Busom Descarrega, J., Sagalowicz, L., & Devezeaux de Lavergne, M. (2024). Understanding mechanisms behind the oily mouthcoating perception of pure vegetable oils using tribology. *55*(2), Article e12829.

Tenorio-Garcia, E., Araiza-Calahorra, A., Rappolt, M., Simone, E., & Sarkar, A. (2023). Pickering water-in-oil emulsions stabilized solely by fat crystals. *Advanced Materials Interfaces, 10*(31), Article 2300190.

Tenorio-Garcia, E., Araiza-Calahorra, A., Simone, E., & Sarkar, A. (2022). Recent advances in design and stability of double emulsions: Trends in Pickering stabilization. *Food Hydrocolloids, 128*, Article 107601.

Tenorio-Garcia, E., Rappolt, M., Sadeghpour, A., Simone, E., & Sarkar, A. (2024). Fabrication and stability of dual pickering double emulsions stabilized with food-grade particles. *Food Hydrocolloids, 156*, Article 110327.

Wang, Q., Zhu, Y., & Chen, J. (2021a). Development of a simulated tongue substrate for in vitro soft "oral" tribology study. *Food Hydrocolloids, 120*, Article 106991.

Wang, Q., Zhu, Y., Ji, Z., & Chen, J. (2021b). Lubrication and sensory properties of emulsion systems and effects of droplet size distribution. *Foods, 10*(12), Article 3024.
You, K.-M., Murray, B. S., Connell, S. D., & Sarkar, A. (2024). Fabrication and lubrication performance of sustainable pickering-like water-in-water emulsions using plant protein microgels. *5*(4), Article 2300160.
You, K.-M., Murray, B. S., & Sarkar, A. (2023). Tribology and rheology of water-in-water emulsions stabilized by whey protein microgels. *Food Hydrocolloids, 134*, Article 108009.
Zembyla, M., Lazidis, A., Murray, B. S., & Sarkar, A. (2019). Water-in-oil Pickering emulsions stabilized by synergistic particle–particle interactions. *Langmuir, 35*(40), 13078–13089.